

Multi-potential capacity for reinforced concrete members under pure torsion

Hyunjin Ju^{1a}, Sun-Jin Han^{2b}, Kang Su Kim^{*2}, Alfred Strauss^{1c} and Wei Wu^{1d}

¹Department of Civil Engineering and Natural Hazards, University of Natural Resources and Life Sciences
Feistmantelstraße 4, 1180 Vienna, Austria

²Department of Architectural Engineering, University of Seoul,
163 Seoulsiripdae-ro, Dongdaemun-gu, Seoul 02504, Republic of Korea

(Received September 7, 2019, Revised February 19, 2020, Accepted March 5, 2020)

Abstract. Unlike the existing truss models for shear and torsion analysis, in this study, the torsional capacities of reinforced concrete (RC) members were estimated by introducing multi-potential capacity criteria that considered the aggregate interlock, concrete crushing, and spalling of concrete cover. The smeared truss model based on the fixed-angle theory was utilized to obtain the torsional behavior of reinforced concrete member, and the multi-potential capacity criteria were then applied to draw the capacity of the member. In addition, to avoid any iterative calculation in the existing torsional behavior model, a simple strength model was suggested that considers key variables, such as the effective thickness of torsional member, principal stress angle, and strain effect that reduces the resistance of concrete due to large longitudinal tensile strain. The proposed multi-potential capacity concept and the simple strength model were verified by comparing with test results collected from the literature. The study found that the multi-potential capacity could estimate in a rational manner not only the torsional strength but also the failure mode of RC members subjected to torsional moment, by reflecting the reinforcing index in both transverse and longitudinal directions, as well as the sectional and material properties of RC members.

Keywords: multi-potential capacity; failure criteria; reinforced concrete; torsion; strength model

1. Introduction

The torsional moment in the design of reinforced concrete members is no longer rare, because some recent buildings are designed with irregular shapes, and structural members also have various geometry (Ju *et al.* 2015, 2019, Tsampras *et al.* 2016, Zhang *et al.* 2018). With the development of concrete technology and material engineering, the structural members can also be designed as a thin and efficient shape to resist external loads, but in such members, there can be various types of loading that combine with each other. Thus, the accurate analysis model for reinforced concrete (RC) member subjected to torsional moment can make the structural design more safe and reliable. In particular, the accurate estimation of capacity and failure mode of RC members would be very helpful to design the members subjected to torsion with other types of loads such as flexure and shear, because it is an uncommon case for a member to be subjected to pure torsional moment. But as the first step to investigate the RC members

subjected to various loads with torsional moment, it is important to identify the torsional resistance mechanism of RC members under pure torsion (Greene and Belarbi 2009, Chalioris 2006).

To this end, there have been various efforts to develop an analytical model for the torsional member. As a classical method, the skew-bending theory (Elfgren *et al.* 1974, Hsu 1984, Lessig 1959) has been developed to define the capacity of reinforced concrete members subjected to not only torsional moment but also combined loads that include bending moment and shear force. However, the analytical models based on skew bending theory have considered only force equilibrium condition, with the assumption of the yielding of reinforcement. Therefore, it is difficult to apply those models to the over-reinforced concrete members which fail in compression. Those models also cannot take into account the tensile resistance and shear contribution of concrete, which have been found to be the most important resistance mechanisms of reinforced concrete members subjected to shear and torsion. In order to overcome these limitations, the variable angle truss model (Hsu and Mo 1985, 2010, Hsu and Zhang 1997, Jeng and Hsu 2009, Ju *et al.* 2013, Lu and Wu 2001, Mitchell and Collins 1974, Pang and Hsu 1996, Rahal and Collins 1995, 1996, Vecchio and Collins 1986) has been developed and further advanced, in which the behavior of RC members can be analyzed considering the compatibility conditions, as well as the force equilibrium. In most truss models, the point where the principal compressive strain reaches the ultimate strain is assumed as the termination point of analysis. However, since member failure is not governed by such a single criterion, the truss models cannot reflect the actual shear

*Corresponding author, Ph.D., Professor

E-mail: kangkim@uos.ac.kr

^a Post-doctoral Research Fellow

E-mail: hyunjin.ju@boku.ac.at

^b Post-doctoral Research Fellow

E-mail: sjhan1219@gmail.com

^c Associate Professor

E-mail: alfred.strauss@boku.ac.at

^d Professor

E-mail: wei.wu@boku.ac.at

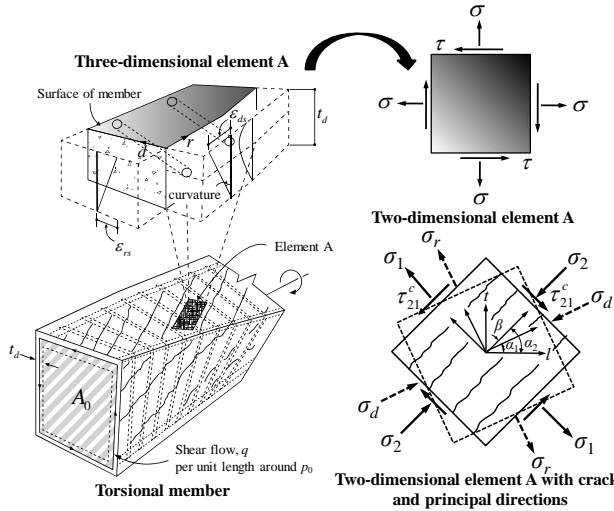


Fig. 1 Reinforced concrete members with rectangular section subjected to torsional moment

and torsional resistance mechanisms of RC members subjected to combined loadings, where there are several failure modes according to the material properties, reinforcement details, and member dimensions.

Therefore, this study presents new failure criteria, so-called multi-potential capacity, in order to consider the complex failure mechanism affected by various stress states due to external loads. Unlike the existing torsional analytical models (Mitchell and Collins 1974, Hsu and Mo 1985, Jeng and Hsu 2009), the multi-potential capacity was derived at the level of stress, so that it can estimate whether the stress state due to external forces reaches the failure point or not. The failure criteria were applied to the existing torsional behavior model to determine the strength of a member subjected to torsional moment. In addition, a simple torsional strength model was also presented by utilizing such failure criteria.

2. Multi-Potential capacity

Since steel material exhibits ductile behavior after yielding, it would be reasonable to define the capacity of reinforced concrete members as the failure of brittle concrete material. The torsional members with rectangular section can be assumed to be subjected to shear stress within the outermost perimeter due to shear flow (q) caused by torsional moment, as shown in Fig. 1 (Hsu 1984), and the three-dimensional element can also be averaged within the shear flow zone as two-dimensional panel element, which is similar to the web shear element of the RC member. When the RC member is subjected to shear stress, the web element of the member is under the biaxial stress state in principal compressive and tensile directions, as presented in Fig. 2(a) (Hwang *et al.* 2016). In this member, the failure can be assumed to occur when one of the principal stresses reaches the material strength, as in the Rankine's failure criteria (Chen 1982) shown in Fig. 2(b).

In more detail, failure occurs when the crack width significantly develops due to large tensile strain, which is

related to aggregate interlock (Sherwood *et al.* 2007, Taylor 1970, Walraven 1981, Watanabe and Lee 1998), or when the concrete crushing occurs due to large compressive stress (Collins and Mitchell 1991). There are also similar approaches which take into account aggregate interlock and concrete crushing in analysis of reinforced concrete member under shear and torsion (Bellett *et al.* 2001, 2017, Cerioni 2011). In addition, the torsional RC member with large cover thickness can fail by concrete spalling (Rahal 1993), and thus it is necessary to define the failure criterion for such members. In this study, the multi-potential capacity criteria that consider the aggregate interlock, concrete crushing, and spalling of concrete cover were proposed to estimate the capacity of RC members subjected to torsional moment.

2.1 Aggregate interlock

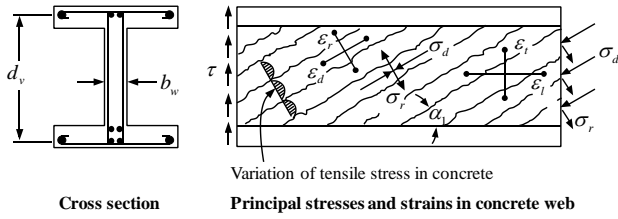
The modified compressive field theory (MCFT) (Vecchio and Collins 1986, 1988) and the disturbed stress field model (Vecchio 2000) explain that the external shear forces acting on RC members are resisted by the cracked concrete web, and the critical shear crack theory (CSCT) (Muttoni and Fernández 2008, Vas Rodrigues *et al.* 2010) also suggests that the shear capacity of RC members should be estimated based on the shear contribution of concrete at crack surface. Therefore, the shear resistance of concrete at the crack surface is regarded as one of the failure criteria, for which the potential shear capacity at the crack surface (τ_{cap}^{ci}), suggested by Vecchio and Collins (1986), was adopted. The potential capacity (τ_{cap}^{ci}) was derived based on the test results reported by Walraven (1981), and can be expressed as follows:

$$\tau_{cap}^{ci} = \frac{0.18\lambda\sqrt{f'_c}}{0.31 + \frac{24w_s}{a_{g,max} + 16}} \quad (\text{MPa}) \quad (1)$$

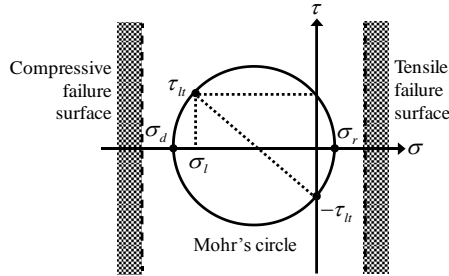
where λ is taken to be 1.0 and 0.75 for normal weight concrete and lightweight aggregate concrete, respectively, w_s is the shear crack width (mm), and $a_{g,max}$ is the maximum size of aggregate (mm), taken as zero for lightweight aggregate concrete (Sherwood *et al.* 2007, Bentz *et al.* 2006), and taken as $a_{g,max} - 0.16f'_c$ (mm) for normal weight aggregate concrete when the compressive strength of concrete exceeds 40 MPa. The aggregate interlock capacity of Equation (1) is a function of crack width (w_s), and the capacity decreases as the crack width increases. Here, the shear crack width can be calculated by multiplying the shear crack spacing ($s_{m\theta}$) by the average tensile strain in the crack direction (ε_1), as follows:

$$w_s = s_{m\theta}\varepsilon_1 \quad (\text{mm}) \quad (2)$$

In fact, the tensile strain at ultimate state is relatively large compared to the cracking strain of concrete, and thus the concrete contribution by tensile stress to the member strength is very small. However, if the member is appropriately reinforced, such large tensile strain and crack width can be controlled by the reinforcement. Collins and



(a) Reinforced concrete members subjected to shear stresses



(b) Rankine's failure criteria (Chen 1982)

Fig. 2 Concept of failure criteria

Mitchell (1991) have suggested an equation for the shear crack spacing by reflecting the role of the reinforcement that controls the crack width, as follows:

$$s_{m\theta} = \frac{1}{(\sin \alpha_2 / s_{mx} + \cos \alpha_2 / s_{mv})} \quad (\text{mm}) \quad (3)$$

where s_{mx} and s_{mv} are the average crack spacing in the longitudinal and transverse direction, respectively, and they are calculated considering the reinforcement details (Collins and Mitchell 1991). In addition, α_2 is the angle of the initial crack with respect to the longitudinal axis.

The required shear stress at the crack surface is defined as the shear stress of concrete at the initial crack surface (τ_{21}^c) in the fixed angle model (Pang and Hsu 1996, Hsu and Zhang 1997, Hsu 1998), as presented in the shear element of Fig. 1. If the τ_{21}^c is larger than the shear resistance capacity (τ_{cap}^{ci}) of Equation (1), the member is regarded to reach the maximum strength by the aggregate interlock mechanism.

2.2 Concrete crushing

When the principal compressive stress exceeds the compressive strength of concrete (f_c'), concrete crushing occurs, and it is considered as one of the failure mechanisms. The compressive stress behavior of cracked concrete subjected to biaxial stress is affected by the softening phenomenon (Belarbi and Hsu 1991, 1995, Hsu and Zhang 1996, Stevens *et al* 1991, Vecchio and Collins 1982, 1993), in which the maximum compressive strength of concrete ($f_{c,max}$) decreases because of the influence of tensile strain. Therefore, the effective compressive strength of concrete can be expressed as $\zeta f_c'$, considering the softening coefficient (ζ) (Vecchio and Collins 1986). The required average compressive stress within the effective thickness of the shear flow zone of the torsional member can be calculated as follows:

$$\sigma_d = k_c \zeta f_c' \quad (\text{MPa}) \quad (4)$$

where k_c is the ratio of the average compressive stress to the peak compressive stress in the concrete strut (Hsu 1984), which can be obtained by integrating the compressive stress-strain curve with respect to the compressive strain through the effective depth (t_d), and then normalizing by the maximum compressive stress and the maximum principal compressive strain (ϵ_{ds}). In addition, the capacity should also be expressed as an average value, however, the Vecchio and Collins' softening coefficient shows a tendency to sharply decrease with increasing principal tensile strain (ϵ_r). Thus, the capacity for concrete crushing was proposed simply with the average coefficient of unit, as follows:

$$\sigma_{cap}^c = 1.0 \zeta f_c' \quad (\text{MPa})$$

$$\text{where } \zeta = \frac{1}{(0.8 + 170 \epsilon_r)} \leq 1.0 \quad (5)$$

The concrete crushing failure mode should be considered to prevent the web concrete crushing or to control the crack width caused by an excessive amount of reinforcement, as specified in major codes, such as ACI 318 (2014) and CSA (2004). Therefore, it would be a basis for limiting the maximum amount of reinforcement (Chakraborty 1977, Chiu *et al.* 2007, Hsu 1968).

Meanwhile, according to the experimental results of the torsional members subjected to axial force reported by Bishara and Peir (1968), when the ratio of the compressive stress to the compressive strength of concrete (σ_{cn}/f_c') exceeds 0.65, so-called transformation point, the torsional strength sharply decreases. This is probably because of concrete crushing caused by softening effect before the compressive strength. Thus, the failure criterion for concrete crushing would also be important to estimate the torsional strength of RC members subjected to axial forces.

2.3 Spalling

The torsional RC members can fail by spalling within the concrete cover outside the closed stirrups. Rahal and Collins (1995) explained the spalling failure mechanism in the RC members subjected to torsion with the consideration of the compressive stress within the cover thickness, the tensile resistance of concrete, and the effective resistance area of concrete. In this study, this spalling potential was adopted to check the failure caused by spalling due to the excessive cover thickness as follows:

$$Sp = \frac{K_1 \int^{cover} \sigma_d dx}{\sqrt{f_c'} w_{sh}} \geq 0.056 \quad (6)$$

where w_{sh} is the effective width resisting horizontal or vertical shear stress. When the spalling potential exceeds the limit value of 0.056, it is assumed that the member has a spalled section. In Equation (6), the principal compressive stress (σ_d) should be integrated along the clear cover only.

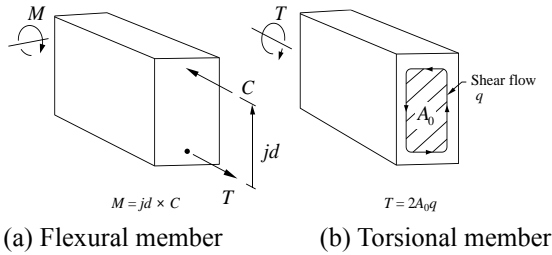


Fig. 3 Analogous concept of torsion to bending

For the horizontal walls of the rectangular section, the integration is performed in the vertical direction and w_{sh} equals the effective depth (d_v) that resists vertical shear. Otherwise, the integration is performed in the horizontal direction and w_{sh} equals the effective width (b_v) that resists horizontal shear stress. For simplicity and conservative purpose, d_v and b_v are replaced by h and b , respectively. Equation (6) is a dimensionless index, and consists of the applied compressive stress within the clear cover, the tensile resistance of concrete ($\sqrt{f'_c}$), and the ratio of the area occupied by the reinforcing bars to the total area along the perimeter of the stirrups (K_1), which can be approximately expressed as follows:

$$K_1 = \frac{\sum d_{bl}s + d_{br}p_h}{p_h s} \quad (7)$$

where d_{bl} is the diameter of longitudinal steel bar, and the summation ($\sum d_{bl}$) is taken over all the bars in contact with the stirrups. In addition, d_{br} is the diameter of the stirrups, p_h is the perimeter of the centerline of the closed stirrups, and s is the spacing of transverse reinforcement.

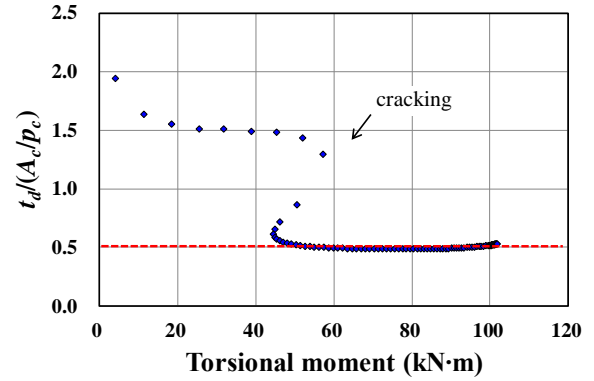
The original spalling criterion considers the partially spalling section according to the loading ratio of the torsional moment to the shear force. However, the criterion has been modified to obtain the member strength on the safe side, by which the member reaches its maximum strength when spalling occurs.

3. Simple strength model

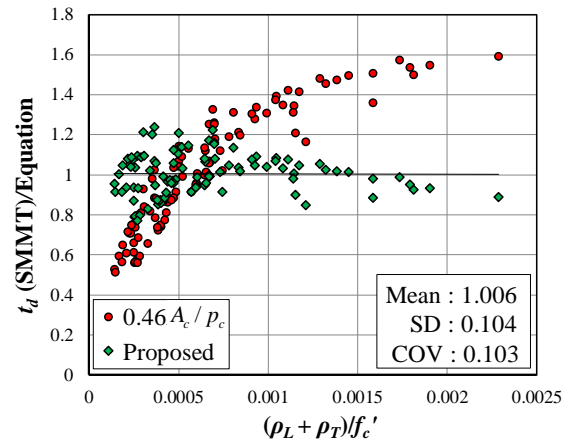
The multi-potential capacity, as described above, is applied to the fixed angle softened truss model (Hsu 1998, Hsu and Zhang 1996, 1997), in order to determine the termination of analysis and the maximum strength of RC members subjected to torsional moment. This study focused on the strength and failure mode of the RC members under pure torsion, for which a simplified truss model is suggested using the multi-potential capacity.

3.1 Effective thickness

The torsional moment is considered to be resisted by the shear flow in a thin-walled tube with the effective thickness (t_d) (Hsu 1984, Bredt 1896) and can be calculated by multiplying the effective thickness by the area enclosed by the centerline of the shear flow zone (A_0), as shown in Fig. 1. Moreover, A_0 is a function of t_d , and thus the effective



(a) Normalized effective thickness and the simple equation



(b) Comparison of Rahal and Collins's equation (1996) and the proposed equations

Fig. 4 Simple equations for torsional variables

thickness, t_d , is a very important variable in the torsional analysis and strength estimation of RC members.

Meanwhile, as shown in Fig. 3, the t_d , A_0 , and T in the torsion are analogous to the depth of neutral axis (c_y), moment arm (j_d), and bending moment (M) in the flexure, respectively (Hsu 1990, Hsu and Mo 2010, Jeng 2015, Mitchell and Collins 1974, Rahal 2001). Therefore, if it is possible to directly calculate the effective thickness (t_d) as in the calculation of flexural strength, where the depth of neutral axis (c_y) is firstly calculated through the force equilibrium, it would be very easy to simplify the calculation of the torsional strength.

According to the simple model by Rahal and Collins (1996), the effective thickness (t_d) is calculated by a function of A_c/p_c , and they have proposed it as $0.46 A_c/p_c$, where A_c is the area enclosed by the outer perimeter of the cross-section, and p_c is the perimeter of the outer concrete cross section. The smeared membrane model for torsion (SMMT) proposed by Jeng and Hsu (2009) was used to obtain the effective thickness of the test specimens under pure torsion presented in Table 1, because it has been known as a relatively accurate analytical model to evaluate the behavior of RC members under pure torsion. Fig. 4(a) presents an analysis example of the relation between the effective thickness and torsional moment, in which after torsional cracking up to the ultimate state, the almost

Table 1 Database of RC specimens subjected to pure torsion

Researcher	Specimen Name	b (mm)	h (mm)	f'_c (MPa)	f_{yt} (MPa)	f_{ys} (MPa)	A_L (mm ²)	A_T (mm ²)	x_0 (mm)	y_0 (mm)	s (mm)	c (mm)	s_x (mm)	c_x (mm)	c_y (mm)	T_u (kN·m)
McMullen and Rangan (1978)	A1	254	254	39.6	360	285	285.2	32	222	222	79.4	13	218	104	108	13.1
	A1R	254	254	36.9	360	285	285.2	32	222	222	79.4	13	215	104	108	12.5
	A2	254	254	38.2	380	285	506.8	32	222	222	41.2	13	212	101	108	22.6
	A3	254	254	39.4	352	360	794.4	32	219	219	79.4	15	206	96.5	106.5	27.8
	A4	254	254	39.2	351	360	1146	32	219	219	57.15	15	215	93.5	106.5	34.5
	B1	178	356	39.9	360	285	285.2	32	146	324	82.55	13	142	155	70	12.8
	B1R	178	356	36.3	360	285	285.2	32	146	324	82.55	13	139	155	70	12.3
	B2	178	356	39.6	380	285	506.8	32	146	324	44.45	13	136	152	70	20.8
	B3	178	356	38.6	352	360	794.4	32	143	321	82.55	15	130	147.5	68.5	25.3
	B4	178	356	38.5	351	360	1146	32	143	321	60.32	15	130	144.5	68.5	31.8
B1	254	381	27.57	313.7	341.2	506.8	71.3	215.9	342.9	152.4	14.05	212.9	163.45	102.95	22.26	
B2	254	381	28.61	316.4	319.9	794.4	126.7	215.9	342.9	181.0	12.55	212.9	161.95	101.45	29.26	
B3	254	381	28.06	327.5	319.9	1146	126.7	215.9	342.9	127.0	12.55	209.9	158.95	101.45	37.51	
B4	254	381	30.54	319.9	323.3	1548	126.7	215.9	342.9	92.1	12.55	206.9	155.95	101.45	47.34	
B5	254	381	29.02	332.3	321.2	2040	126.7	215.9	342.9	69.9	12.55	203.9	152.95	101.45	56.15	
B6	254	381	28.82	331.6	322.6	2580	126.7	215.9	342.9	57.2	12.55	199.9	148.95	101.45	61.69	
B7	254	381	25.99	319.9	318.5	506.8	126.7	215.9	342.9	127.0	12.55	215.9	164.95	101.45	26.89	
B8	254	381	26.75	321.9	319.9	506.8	126.7	215.9	342.9	57.2	12.55	215.9	164.95	101.45	32.54	
B9	254	381	28.82	319.2	342.6	1146	71.3	215.9	342.9	152.4	14.05	206.9	157.45	102.95	29.83	
B10	254	381	26.47	334.3	341.9	2580	71.3	215.9	342.9	152.4	14.05	196.9	147.45	102.95	34.35	
M1	254	381	29.85	326.1	353	794.4	71.3	215.9	342.9	149.2	14.05	209.9	160.45	102.95	30.39	
M2	254	381	30.54	328.8	357.1	1146	71.3	215.9	342.9	104.7	14.05	206.9	157.45	102.95	40.56	
M3	254	381	26.75	321.9	326.1	1548	126.7	215.9	342.9	139.7	12.55	206.9	155.95	101.45	43.84	
M4	254	381	26.54	318.5	326.8	2040	126.7	215.9	342.9	104.8	12.55	203.9	152.95	101.45	49.6	
M5	254	381	27.99	335	330.9	2580	126.7	215.9	342.9	82.6	12.55	199.9	148.95	101.45	55.7	
M6	254	381	29.37	317.8	340.6	3060	126.7	215.9	342.9	69.9	12.55	203.9	152.95	101.45	60.1	
I2	254	381	45.22	325.4	348.8	794.4	71.3	215.9	342.9	98.4	14.05	209.9	160.45	102.95	36.04	
I3	254	381	44.74	343.3	333.7	1146	126.7	215.9	342.9	127.0	12.55	209.9	158.95	101.45	45.64	
I4	254	381	45.36	315	326.1	1548	126.7	215.9	342.9	92.1	12.55	206.9	155.95	101.45	58.07	
I5	254	381	45	310	325.4	2040	126.7	215.9	342.9	69.9	12.55	203.9	152.95	101.45	70.72	
I6	254	381	45.78	325.4	328.8	2580	126.7	215.9	342.9	57.2	12.55	199.9	148.95	101.45	76.71	
J1	254	381	14.34	327.5	346.1	506.8	71.3	215.9	342.9	152.4	14.05	212.9	163.45	102.95	21.47	
J2	254	381	14.54	319.9	340.6	794.4	71.3	215.9	342.9	98.4	14.05	209.9	160.45	102.95	29.15	
J3	254	381	16.89	338.5	337.1	1146	126.7	215.9	342.9	127.0	12.55	209.9	158.95	101.45	35.25	
J4	254	381	16.75	324	331.6	1548	126.7	215.9	342.9	92.1	12.55	206.9	155.95	101.45	40.67	
G1	254	508	29.78	321.9	339.2	506.8	71.3	215.9	469.9	187.3	14.05	212.9	226.95	102.95	26.78	
G2	254	508	30.88	322.6	333.7	794.4	71.3	215.9	469.9	120.7	14.05	209.9	223.95	102.95	40.33	
G3	254	508	26.82	338.5	327.5	1146	126.7	215.9	469.9	155.6	12.55	209.9	222.45	101.45	49.6	
G4	254	508	28.26	325.4	321.2	1548	126.7	215.9	469.9	114.3	12.55	206.9	219.45	101.45	64.85	
G5	254	508	26.88	330.9	327.5	2040	126.7	215.9	469.9	85.7	12.55	203.9	216.45	101.45	71.97	
G6	254	508	29.92	334.3	349.5	760.2	71.3	215.9	469.9	127.0	14.05	212.9	226.95	102.95	39.09	
G7	254	508	30.95	319.2	322.6	1191.6	126.7	215.9	469.9	146.1	14.05	209.9	223.95	102.95	52.65	
G8	254	508	28.33	321.9	328.8	1719	126.7	215.9	469.9	104.8	14.05	206.9	220.95	102.95	73.44	
N1	152	304	29.5	352.3	341.2	285.2	32	130.3	282.7	92.1	7.65	126.7	134.35	62.35	9.09	
N1a	152	304	28.68	346.1	344.7	285.2	32	130.3	282.7	92.1	7.65	126.7	134.35	62.35	8.99	
N2	152	304	30.4	330.9	337.8	506.8	32	130.3	282.7	50.8	7.65	123.7	131.35	62.35	14.46	
N2a	152	304	28.4	333	360.5	506.8	71.3	130.3	282.7	114.3	5.65	127.7	133.35	60.35	13.22	
N3	152	304	27.3	351.6	351.6	427.8	32	130.3	282.7	63.5	7.65	126.7	134.35	62.35	12.2	
N4	152	304	27.3	337.1	355.7	649.4	71.3	130.3	282.7	88.9	5.65	127.7	133.35	60.35	15.7	
K1	152	495	29.85	345.4	354.3	427.8	71.3	114.3	457.2	190.5	13.9	114.2	223.6	52.1	15.37	
K2	152	495	30.61	335.7	337.8	760.2	71.3	114.3	457.2	104.8	13.9	111.2	220.6	52.1	23.73	
K3	152	495	29.02	315.7	320.6	1191.6	126.7	114.3	457.2	123.8	12.4	111.2	219.1	50.6	28.47	
K4	152	495	28.61	344	339.9	1719	126.7	114.3	457.2	85.7	12.4	108.2	216.1	50.6	35.02	
C1	254	254	27.02	341.2	341.2	285.2	71.3	215.9	215.9	215.9	14.05	215.9	102.95	102.95	11.3	
C2	254	254	26.54	334.3	344.7	506.8	71.3	215.9	215.9	117.5	14.05	212.9	99.95	102.95	15.25	
C3	254	254	26.88	330.9	329.5	794.4	126.7	215.9	215.9	139.7	12.55	212.9	98.45	101.45	20	
C4	254	254	27.16	336.4	327.5	1146	126.7	215.9	215.9	98.4	12.55	209.9	95.45	101.45	25.31	
C5	254	254	27.23	328.1	328.8	1548	126.7	215.9	215.9	73.0	12.55	206.9	92.45	101.45	29.71	
C6	254	254	27.57	315.7	327.5	2040	126.7	215.9	215.9	54.0	12.55	203.9	89.45	101.45	34.23	
Koutchoukali and Belarbi (2001)	B5UR1	203	305	39.6	386	373	506.8	71.3	165	267	108	14	162	125.5	77.5	19.4
	B7UR1	203	305	64.6	386	399	506.8	71.3	165	267	108	14	162	125.5	77.5	18.9
	B9UR1	203	305	75	386	373	506.8	71.3	165	267	108	14	162	125.5	77.5	21.1
	B12UR1	203	305	80.6	386	399	506.8	71.3	165	267	108	14	162	125.5	77.5	19.4
	B14UR1	203	305	93.9	386	386	506.8	71.3	165	267	108	14	162	125.5	77.5	21
	B12UR2	203	305	76.2	386	386	506.8	71.3	165	267	102	14	162	125.5	77.5	18.4
	B12UR3	203	305	72.9	373	386	649.4	71.3	165	267	95	14	162	125.5	77.5	22.5
	B12UR4	203	305	75.9	373	386	760.2	71.3	165	267	90	14	162	125.5	77.5	23.7
B12UR5	203	305	76.7	380	386	794.4	71.3	165	267	70	14	159	122.5	77.5	24	

Table 1 Continued

Researcher	Specimen Name	b (mm)	h (mm)	f'_c (MPa)	f_{yl} (MPa)	f_{yt} (MPa)	A_{le} (mm ²)	A_T (mm ²)	x_0 (mm)	y_0 (mm)	s (mm)	c (mm)	s_x (mm)	c_x (mm)	c_y (mm)	T_u (kN·m)
Fang and Shiau (2004)	H-06-06	350	500	78.5	440	440	1191	71.3	300	450	100	20	294	214	145	92
	H-06-12	350	500	78.5	410	440	2027	71.3	300	450	100	20	92	217	145	115.1
	H-12-12	350	500	78.5	410	440	2027	71.3	300	450	50	20	92	217	145	155.3
	H-12-16	350	500	78.5	520	440	2865	71.3	300	450	50	20	145	211	145	196
	H-20-20	350	500	78.5	560	440	3438	126.7	300	450	55	19	147	212	143	239
	H-07-10	350	500	68.4	500	420	1719	71.3	300	450	90	20	291	211	145	126.7
	H-14-10	350	500	68.4	500	360	1719	71.3	300	450	80	20	291	211	145	135.2
	H-07-16	350	500	68.4	500	420	2865	71.3	300	450	90	20	145	211	145	144.5
	N-06-06	350	500	35.5	440	440	1191	71.3	300	450	100	20	294	214	145	79.7
	N-06-12	350	500	35.5	410	440	2027	71.3	300	450	100	20	92	217	145	95.2
	N-12-12	350	500	35.5	410	440	2027	71.3	300	450	50	20	92	217	145	116.8
	N-12-16	350	500	35.5	520	440	2865	71.3	300	450	50	20	145	211	145	138
	N-20-20	350	500	35.5	560	440	3438	126.7	300	450	55	19	147	212	143	158
	N-07-10	350	500	33.5	500	420	1719	71.3	300	450	90	20	291	211	145	111.7
	N-14-10	350	500	33.5	500	360	1719	126.7	300	450	80	19	294	212	143	125
N-07-16	350	500	33.5	500	420	2865	71.3	300	450	90	20	145	211	145	117.3	
Chiu <i>et al.</i> (2007)	NBS-43-44	350	500	35	400	385	760.2	71.3	300	450	13	10	140	20	297	217
	HBS-74-17	350	500	67	505	600	1288.6	32	300	450	19	6	140	22	287	209
	HBS-82-13	350	500	67	493	600	1431.2	32	300	450	19	6	190	22	287	209
	NBS-82-13	350	500	35	493	600	1431.2	32	300	450	19	6	190	22	287	209
	HBS-60-61	350	500	67	402	385	1047.8	71.3	300	450	16	10	100	20	294	214
Lee and Kim (2010)	T1-1	300	350	43.15	410	2.05	506.8	71.3	260	310	130	15	257	147	125	32.86
	T1-2	300	350	44.04	410	2.05	760.2	71.3	260	310	85	15	257	147	125	45.89
	T1-3	300	350	41.7	410	2.05	1013.6	71.3	260	310	65	15	128.5	147	125	54.05
	T1-4	300	350	42.55	510	2.05	1191.6	126.7	260	310	75	14	257	145.5	123.5	62.41
	T2-1	300	350	40.08	410	2.05	506.8	71.3	260	310	225	15	257	147	125	26.05
	T2-2	300	350	41.7	510	2.05	1191.6	71.3	260	310	130	15	254	144	125	38.11
	T2-3	300	350	42.71	510	2.05	1191.6	71.3	260	310	88	15	254	144	125	50.16
	T2-4	300	350	42.64	512.4	2.05	1400.2	71.3	260	310	75	15	257	147	125	56.39

Note

b : width of section, h : height of section, f'_c : compressive strength of concrete, f_{yl} : yield stress of longitudinal reinforcement, f_{yt} : yield stress of transverse reinforcement, A_{le} : sectional area of one longitudinal steel bar, A_L : total sectional area of longitudinal reinforcement, A_T : area of one leg of stirrups or amount of transverse reinforcement, x_0 : smaller center-to-center dimension of closed stirrup, y_0 : larger center-to-center dimension of closed stirrup, s : spacing of transverse reinforcement, c : thickness of concrete cover, s_x, c_x, c_y : crack width parameters (Collins and Mitchell 1991), T_u : ultimate torsional moment

constant effective thickness can be found. As shown in Fig. 4(b), the effective thickness proposed by Rahal and Collins (1996) provided a considerably accurate result, but it shows an increasing tendency according to the ratio of reinforcement ratio to the compressive strength of concrete. This is because, although the torsional effective thickness should be determined by the force equilibrium between concrete and reinforcement (Hsu 1984, 1990), the Rahal and Collins' equation consider only dimensional variables.

Therefore, the equation proposed by Rahal and Collins (1996) was modified to fit the analyzed effective thickness

reflecting the variable $(\rho_L + \rho_T)/f'_c$, as follows:

$$t_d = 10.6 \frac{A_c}{p_c} \left(\frac{\rho_L + \rho_T}{f'_c} \right)^{0.42} \quad (\text{mm}) \quad (8)$$

where ρ_L and ρ_T are the longitudinal and transverse reinforcement ratios in gross section, which are calculated by A_l/A_c and A_p/A_c , respectively. In addition, A_l and A_p are the amount of longitudinal and transverse reinforcement, respectively. Fig. 4(b) shows the average and

COV of the ratio of the effective thickness by the analysis to that by Equation (8), which were 1.006 and 0.103, respectively. It means a quite good accuracy compared to the Rahal and Collins' equation. It is noted that the effective thickness (t_d) of Equation (8) is limited by $0.75 A_c/p_c$, which is the thickness at the torsional cracking, specified by ACI 318 (2014), to prevent excessive t_d .

3.2 Principal stress angle

The inclination angle of compression strut (α) is another important factor that affects the shear resistance capacity of RC members. In particular, it directly affects the aggregate interlock failure criterion, the magnitude of principal compressive stress in the in-plane shear element, and the subsequent concrete crushing capacity. In addition, the α is also an important variable to determine the contribution of reinforcement in the space truss analogy (Hsu 1984, Lee and Kim 2010). Since it is very difficult to determine the inclination angle of the compression strut without any iterative calculation in the smeared truss models, it can be useful to provide a chart or simple equation to calculate the α , based on a vast amount of parametric analysis results (Bentz and Collins 2004, CSA 2004, Hsu and Mo 1985).

From the behavior analysis of the pure torsional members in Table 1, the principal stress angles at the torsional strength were extracted, and a simple equation for estimating the principal stress angle (α_1) without iterative calculation was proposed considering key variables. The principal stress angle (α_1) calculated using the SMMT showed no tendency according to the compressive strength of concrete (f'_c), while a clear tendency can be obtained according to the reinforcement ratio index (ρ_{index}), as shown in Fig. 5, and thus the principal stress angle (α_1) has been simplified as follows:

$$\alpha_1 = 36^\circ + 12\rho_{index} - 2.5\rho_{index}^2 \quad (9)$$

$$\text{where } \rho_{index} = \frac{\rho_T f_{ly}}{\rho_L f_{ly}} \leq 2.4$$

where f_{ly} and f_{ly} are the yield strength of longitudinal and transverse reinforcement, respectively, and ρ_{index} is limited to 2.4. The initial crack angle (α_2) was taken as 45 degrees because in the case of the RC member subjected to pure torsion, the concrete web element experiences pure shear stress state (Hsu and Zhu 2002, Jeng and Hsu 2009).

3.3 Strain effect

The shear and torsional strength of RC members are affected by various factors, such as member dimension, material properties, and type of loadings. As the longitudinal strain (ε_x) of the member increases due to loading, the crack width increases, and the aggregate interlock capacity, which is regarded as the main shear resistance contribution in MCFT, decreases. This phenomenon is termed the "strain effect" (Bentz and Collins 2006). Therefore, the shear provision of the Canadian code (CSA 1994), which is based on MCFT, has taken the longitudinal strain (ε_x) as a key parameter,

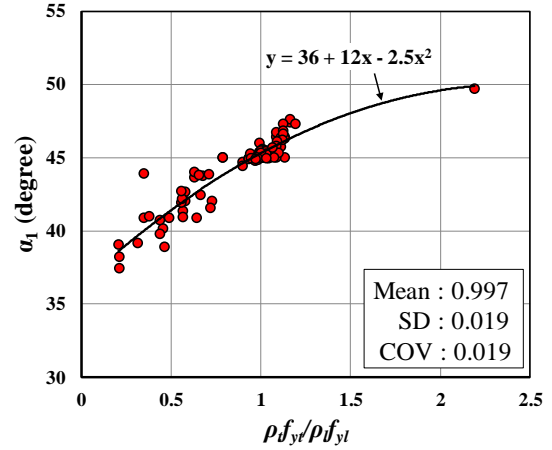


Fig. 5 Principal stress angles versus reinforcement indices

considering the stiffness of longitudinal reinforcement and applied loadings, to calculate the shear capacity of RC members (Rahal and Collins 1999).

The longitudinal strain (ε_l) due to torsional moment is calculated by dividing the longitudinal force (F_L) generated by torsion by the axial stiffness of the reinforcement. The longitudinal force (F_L) of the RC member under pure torsion can be derived from the force equilibrium of the space truss model (Hsu 1984, Wight 2015) as follows:

$$F_L = A_t f_l = \frac{qp_0}{\tan \alpha_1} = \frac{T}{2A_0} p_0 \cot \alpha_1 \quad (10)$$

where f_l is the stress of longitudinal reinforcement, and p_0 is the perimeter of the shear flow resultant. The longitudinal strain (ε_l) can be obtained as follows:

$$\varepsilon_l = \frac{T p_0 \cot \alpha_1}{2A_0 A_t E_s} \quad (11)$$

where E_s is the elastic modulus of steel reinforcement. Before the yielding of reinforcement, the longitudinal strain calculated by Equation (11) is valid; but after yielding, the embedded steel bars show hardening behavior (Belarbi and Hus 1994). In this study, a simple hardening model (Lee *et al.* 2016) presented in Fig. 6 was used for the stress-strain relationship of reinforcement as follows:

$$f_s = E_s \varepsilon_{st} \quad (12a)$$

$$f_s = f_y + E_{sp} (\varepsilon_{st} - \varepsilon_y) \quad (12b)$$

where ε_{st} is the strain of reinforcement, f_y is the yield strength of reinforcement, ε_y is the yield strain of reinforcement, and E_{sp} is the post-yielding elastic modulus of reinforcement, taken as $0.01E_s$.

3.4 Simplified shear element

With the aforementioned simple equations and strain effect, the shear element of the torsional RC member shown in Fig. 1 is analyzed to obtain the required stress and strain. The equilibrium conditions in the orthogonal directions can

be expressed with principal stress components for simplicity, as follows (Ju *et al.* 2020):

$$\sigma_l = \sigma_d \cos^2 \alpha_1 + \sigma_r \sin^2 \alpha_1 + \rho_l f_l \quad (13)$$

$$\sigma_t = \sigma_d \sin^2 \alpha_1 + \sigma_r \cos^2 \alpha_1 + \rho_t f_t \quad (14)$$

$$\tau_{lt} = (\sigma_r - \sigma_d) \sin \alpha_1 \cos \alpha_1 \quad (15)$$

where ρ_l and ρ_t are the longitudinal and transverse reinforcement ratios in the shear element, and these can be calculated as $A_l/(t_d p_0)$ and $A_l/(t_d s)$, respectively. In addition, f_l and f_t are the stresses of longitudinal and transverse reinforcement, respectively, while τ_{lt} is the shear stress due to torsional moment, which is calculated by $T/(2A_0 t_d)$ (Bredt 1896). In addition, the strain compatibility conditions in the longitudinal, transverse, and principal directions can be expressed as follows (Hsu and Mo 2010):

$$\varepsilon_l + \varepsilon_t = \varepsilon_d + \varepsilon_r \quad (16)$$

Since the principal tensile stress (σ_r) and principal compressive strain (ε_d) are relatively small at the ultimate state, they can be assumed to be negligible. Therefore, by substituting $\sigma_r = 0$ and $\varepsilon_d = 0$ into Equations (13)-(16), the equilibrium and compatibility equations are simplified as follows:

$$\sigma_l = \sigma_d \cos^2 \alpha_1 + \rho_l f_l \quad (17)$$

$$\sigma_t = \sigma_d \sin^2 \alpha_1 + \rho_t f_t \quad (18)$$

$$\tau_{lt} = (-\sigma_d) \sin \alpha_1 \cos \alpha_1 \quad (19)$$

$$\varepsilon_l + \varepsilon_t = \varepsilon_r \quad (20)$$

Assuming no clamping stress ($\sigma_t = 0$), the principal compressive stress (σ_d) and the stress of transverse reinforcement (f_t) are expressed as follows:

$$\sigma_d = \frac{-\tau_{lt}}{\sin \alpha_1 \cos \alpha_1} \quad (21)$$

$$f_t = \frac{-\sigma_d \sin^2 \alpha_1}{\rho_t} \quad (22)$$

The principal compressive stress (σ_d) of Equation (21) is the required stress, which is used to check the concrete crushing failure. In addition, the strain of transverse reinforcement (ε_t) can be obtained from the stress-strain relationship of the reinforcement, as shown in Fig. 6. Here, the principal stress angle (α_1) can be calculated by Equation (9).

The shear stress at the crack surface (τ_{21}^c), which is used to check the aggregate interlock criterion, is calculated by transforming the principal stresses by the deviation angle (β) with the assumption of zero tensile stress of concrete ($\sigma_r = 0$) as follows:

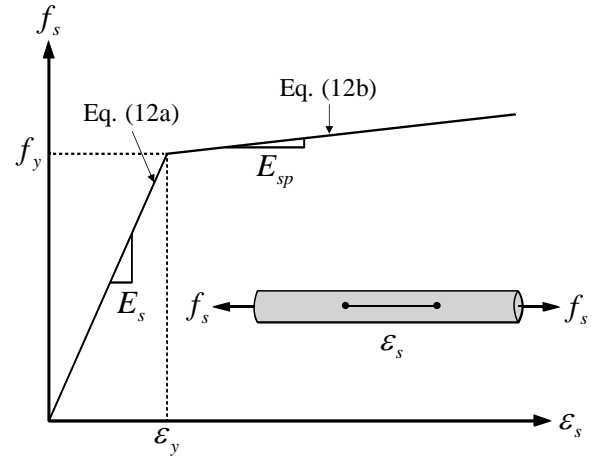


Fig. 6 Stress-strain relationship of steel reinforcement

$$\tau_{21}^c = \sigma_d \sin \beta \cos \beta \quad (23)$$

Since the initial crack angle (α_2) is assumed to be 45 degrees, the deviation angle (β) can be easily calculated with Equation (9) for α_1 as follows:

$$\beta = \alpha_2 - \alpha_1 \quad (24)$$

3.5 Solution algorithm

The analysis procedure is based on the force-controlled process, and it is divided into the preparation step for input, the panel element analysis step, and the failure criteria check step, as below.

1. With the given values, select the initial value for a torsional moment (T) near zero, and calculate the effective thickness of shear flow (t_d) using Equation (8). Then, calculate the shear stress (τ_{lt}) by $T/(2A_0 t_d)$, and average shear crack width (w_s) using Equation (2), where the tensile strain in the crack direction (ε_l) can be expressed by transforming the principal tensile strain by β with the assumption of $\varepsilon_d = 0$, as follows:

$$\varepsilon_l = \varepsilon_r \cos^2 \beta \quad (25)$$

2. Calculate the principal compressive stress (σ_d) by using Equation (21), shear stress at the crack surface (τ_{21}^c) by using Equation (23), and transverse reinforcement (ε_t) by using Equation (20) with the longitudinal strain (ε_l) of Equation (11).

3. Calculate the capacities for aggregate interlock and concrete crushing by using Equations (1) and (5), respectively, and then check whether the required stresses (Equations (23) and (21)) exceed the corresponding capacities or not.

The above process is repeated with increasing the torsional moment until the required stress reaches the corresponding capacity. Since spalling occurs just before maximum load in a few specimens whose cover thickness is excessively large (McMullen and El-Degwy 1985, Rahal 2006), the spalling is not deemed a dominant failure mode in typical torsional RC members. Therefore, in the proposed simple strength model, only the aggregate interlock and

concrete crushing are considered for the multi-potential capacity criteria.

4. Verification of the proposed model

To verify the multi-potential capacity, the criteria were applied to the SMMT so that the strengths of RC members were estimated. The original analysis takes the termination point of analysis when the maximum strain at the surface of the thin-walled tube (ϵ_{ds}) reaches -0.005 (Jeng and Hsu 2009), to obtain sufficient information on the overall behavior, including the descending region after maximum strength. The torsional strengths estimated by the multi-potential capacity criteria were compared with the maximum torsional moment. In addition, the proposed simple strength model was used to calculate the torsional strengths of RC specimens under pure torsion that were collected from the literature, as shown in Table 1.

Fig. 7 compares the experimental results with the calculated torsional strengths, while Table 2 summarizes the estimation results. The average of the ratio of the test results to the maximum torsional moment was 0.937, and the coefficient of variation (COV) was 0.129, while the estimation results with multi-potential capacity (MPC) were 0.966 and 0.147 for the average and COV, respectively. The suggested criteria evaluated the torsional strengths of the specimens on the conservative side and showed almost the same accuracy as the original SMMT. In the case of the simple strength model (SSM), it was found that the average and COV of the ratio of the test results to the calculated torsional strengths were 1.189 and 0.209, respectively, which indicates that the accuracy is somewhat lower than the other estimation results. However, the comparable torsional strength can be simply obtained by using the proposed simple method, while providing failure mode related to the behavioral mechanism.

Fig. 8 shows the analysis results of the failure modes by applying the multi-potential capacity to the SMMT. In the graph, CC, AI, and SP represent the failure modes that are dominated by concrete crushing, aggregate interlock, and spalling, respectively. Since it is unusual for the RC members to have much more transverse reinforcement than longitudinal reinforcement, the specimens with $\rho_T f_{yT} / \rho_L f_{yL} \geq 2.0$ are excluded in the Fig. 8. In the case that $\rho_T f_{yT} / \rho_L f_{yL}$ is close to 1.0, the concrete crushing criterion determined the failure points, while in the specimens with $\rho_T f_{yT} / \rho_L f_{yL} < 0.75$, the aggregate interlock criterion tended to dominate the failure. Meanwhile, four specimens were estimated as spalling failure, because these specimens have a relatively large cover thickness and are subjected to high compressive stress.

Fig. 9 shows the example of the torsional behavior of RC members estimated as aggregate interlock failure and concrete crushing failure. The figures also present how the demand and potential capacity are changed according to the increase in torsional moment. In the analysis of torsional behavior, the failure mode and torsional strength are

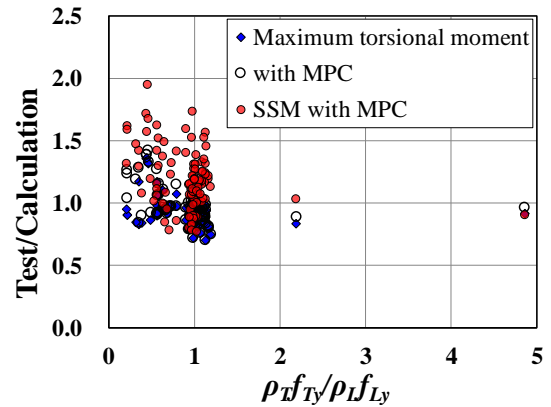


Fig. 7 Comparison of test and analysis results

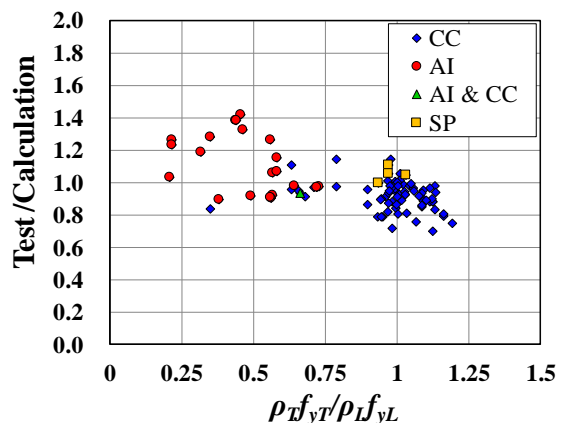


Fig. 8 Failure modes by multi-potential capacity

determined when the required stress reaches one of the criteria.

In the RC member equally reinforced in both directions, the principal stress angle is formed close to 45 degrees regardless of the load, and thus the deviation angle between the principal stress angle and the initial crack angle is about zero. Since the shear stress at the crack surface (τ_{21}^c) is developed depending on the deviation angle (β), in the case of $\beta=0$, there is almost no shear stress at the crack surface. Therefore, the failure due to concrete crushing occurs in that case rather than aggregate interlock failure. In addition, $\beta=0$ means that the initial crack angle is similar to the principal stress angle, which is also consistent with the mechanical explanation that shear stress cannot exist in the principal stress direction (Goodno and Gere 2017).

The principal stress angle deviation from the initial crack angle according to the reinforcement ratio in both directions can be found from the panel tests conducted by Vecchio and Collins (1982). Fig. 10(a) presents the crack patterns of the RC panel specimens subjected to pure shear, in which the ratio of transverse reinforcement is equal to that of longitudinal reinforcement. In such specimens, the initial crack angle was formed at 45 degrees, and the angle of the critical crack causing failure was also formed near 45 degrees. On the other hand, Fig. 10(b) presents the crack patterns of panel specimens where the amount of transverse reinforcement varied, while that of longitudinal reinforcement was kept constant. The ratios of longitudinal

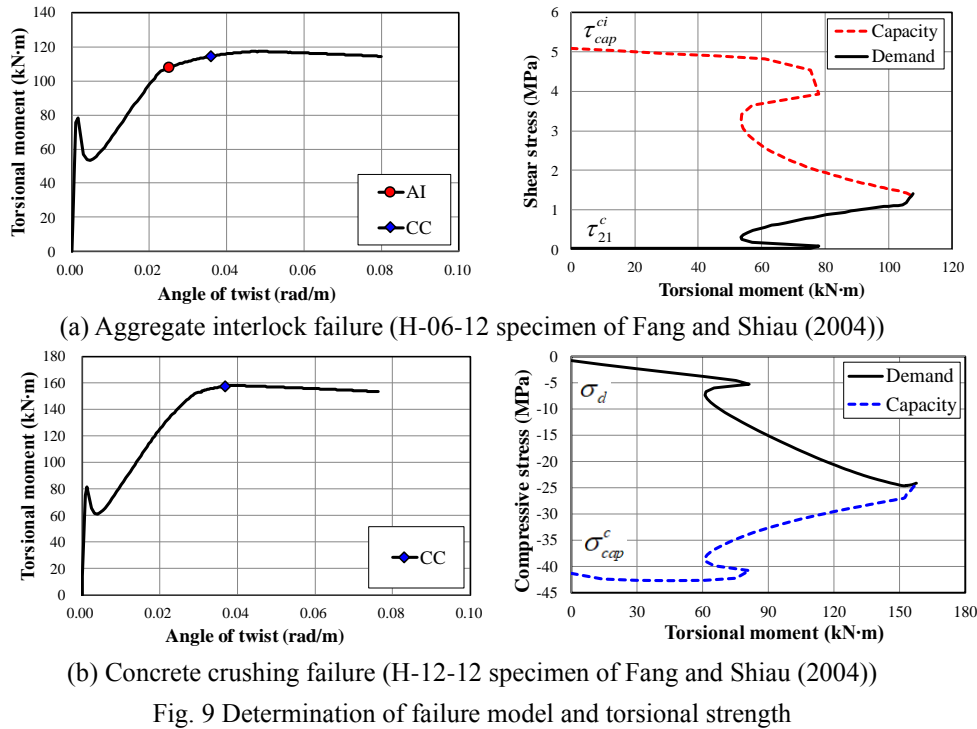


Fig. 9 Determination of failure model and torsional strength

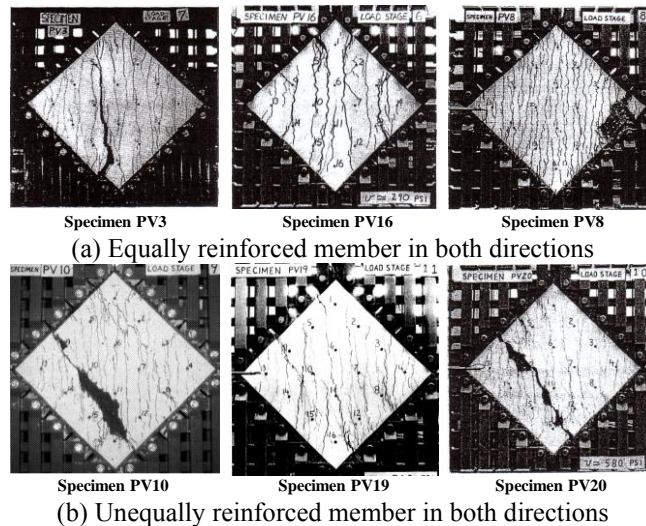


Fig. 10 Crack patterns of panel specimens (Vecchio and Collins 1993)

and transverse reinforcement indices, $\rho_T f_{Ty} / \rho_L f_{Ly}$, of the PV10, PV19, and PV20 specimens were 0.560, 0.261, and 0.324, respectively. The specimens are reinforced more in the longitudinal direction than in the transverse direction. The initial crack angles of the specimens were formed at 45 degrees, but the critical cracks that cause the ultimate failure were formed at an angle close to the longitudinal direction. Although the initial crack is formed at 45 degrees, the unequally reinforced member has the principal stress angle closer to the more reinforced direction according to increasing load.

The multi-potential capacity model provides a rational way to estimate the strengths and failure modes of RC members by reflecting the reinforcing indices in both the transverse and the longitudinal directions as well as their

sectional and material properties. The simple strength estimation model derived in this study utilizing the multi-potential capacity criteria is also expected to be very useful for practical torsional design in the field.

5. Conclusions

In this study, the multi-potential capacity criteria for RC members subjected to torsional moment were presented to determine the strength and failure mode of the members in a rational manner. The multi-potential capacity criteria were applied to the existing torsional behavior model, and a simple strength estimation model with multi-potential capacity criteria was also proposed. In addition, the proposed multi-potential capacity concept and the simple

strength model were verified by comparing with test results collected from the literature. The conclusions of this study are summarized as follows:

- The multi-potential capacity was derived based on the thin-walled tube theory and fixed angle truss model to consider the torsional member as the shear stress element and to reflect the aggregate interlock, concrete crushing, and spalling failure mechanisms.

- The simple strength model with multi-potential capacity was proposed to calculate the member capacity without any complex iterative calculation, in which the simple equations for estimating the effective thickness (t_d) and principal stress angle (α_1) were suggested. In addition, the strain effect was considered to reflect the reduced capacity of the concrete section with larger longitudinal strain.

- The smeared membrane model for torsion was used in order to apply the multi-potential capacity, and the analysis results showed that the multi-potential capacity well provided the point where the member reaches its maximum strength with the high accuracy.

- The multi-potential capacity was also able to determine the failure mode considering the reinforcing indices in both transverse and longitudinal directions, as well as the sectional and material properties of RC members, by which it was confirmed that the behavior mechanism of RC members subjected to shear stress was rationally considered.

- Although the accuracy of the proposed simple strength model is somewhat lower than that of the other detailed analysis models, the torsional strength of RC members can be obtained simply by using the proposed model, and thus it is considered to be applicable to torsional design in practice.

- Since the multi-potential capacity was suggested in the stress level, it would be easily utilized to define the capacity of RC members subjected to various types of loading.

- There are still some issues that need future research, such as failure modes defined in the multi-potential capacity; influencing factors for spalling failure, aggregate interlock capacity according to the aggregate size, tensile behavior of concrete subjected to out-of-plane stress in torsional members.

Acknowledgments

This research was supported by Basic Science Research Program through the National Research Foundation of Korea(NRF) funded by the Ministry of Education(2018R1A6A3A03010707).

References

ACI 318 (2014), Building Code Requirements for Structural Concrete and Commentary. American Concrete Institute, ACI 318R-14, Farmington Hills, MI, USA.

Belarbi, A. and Hsu, T.T.C. (1991), "Constitutive Laws of Concrete in Biaxial Tension-Compression", Research Report UHCEE 91-2; Department of Civil and Environmental

Engineering, University of Houston, Houston, Texas, 1-155.

Belarbi, A. and Hsu, T.T.C. (1994), "Constitutive Laws of Concrete in Tension and Reinforcing Bars Stiffened by Concrete", *ACI Struct. J.*, **91**(4), 465-474. <http://doi.org/10.14359/4154>.

Belarbi, A. and Hsu, T.T.C. (1995), "Constitutive Laws of Softened Concrete in Biaxial Tension-Compression", *ACI Struct. J.*, **92**(5), 562-573. <http://doi.org/10.14359/907>.

Belletti, B., Cerioni, R. and Iori, I. (2001), "Physical Approach for Reinforced-Concrete (PARC) Membrane Elements", *J. Struct. Eng.*, **127**(12), 1412-1426. [https://doi.org/10.1061/\(ASCE\)0733-9445\(2001\)127:12\(1412\)](https://doi.org/10.1061/(ASCE)0733-9445(2001)127:12(1412)).

Belletti, B., Scolari, M. and Vecchi, F. (2017), "PARC_CL 2.0 Crack Model for NLFEA of Reinforced Concrete Structures under Cyclic Loadings", *Comput. Struct.*, **191**(1), 165-179. <https://doi.org/10.1016/j.compstruc.2017.06.008>.

Bentz, E.C. and Collins, M.P. (2006), "Development of the 2004 Canadian Standards Association (CSA) A23.3 Shear Provisions for Reinforced Concrete", *Canadian J. Civil Eng.*, **33**(5), 521-534. <http://doi.org/10.1139/L06-005>.

Bentz, E.C., Vecchio, F.J. and Collins, M.P. (2006), "Simplified Modified Compression Field Theory for Calculating Shear Strength of Reinforced Concrete Elements", *ACI Struct. J.*, **103**(4), 614-624. <http://doi.org/10.14359/16438>.

Bishara, A. and Peir, J.C. (1968), "Reinforced Concrete Rectangular Columns in Torsion", *J. Struct. Division ASCE*, **94**(ST12), 2913-2933.

Bredt, R. (1896), "Kritische Bemerkungen zur Drehungselastizitat. Z Vereines Deutscher Ingenieure", *Band*, **40**(28), 785-790.

Cerioni, R., Bernardi, P., Michelini, E. and Mordini, A. (2011), "A general 3D Approach for the Analysis of Multi-Axial Fracture Behavior of Reinforced Concrete Elements", *Eng. Fracture Mech.*, **78**(8), 1784-1793. <https://doi.org/10.1016/j.engfractmech.2011.01.020>.

Chakraborty, M. (1977), "Torsional-Balanced Steel in Concrete Beams", *J. ASCE Struct. Division*, **103**(ST11), 2181-2191.

Chalioris, C.E. (2006), "Experimental Study of the Torsion of Reinforced Concrete Beams", *Struct. Eng. Mech.*, **23**(6), 713-737. <https://doi.org/10.12989/sem.2006.23.6.713>.

Chen, W.F. (1982), *Plasticity in Reinforced Concrete*, McGraw-Hill, New York, USA.

Chiu, H.J., Fang, I.K., Young, W.T. and Shiau, J.K. (2007), "Behavior of Reinforced Concrete Beams with Minimum Torsional Reinforcement", *Eng. Struct.*, **29**(9), 2193-2205. <https://doi.org/10.1016/j.engstruct.2006.11.004>.

Collins, M.P. and Mitchell, D. (1991), *Prestressed Concrete Structures*, Prentice-Hall, New Jersey, USA.

CSA (1994), Design of concrete structures. A23.3-94, Canadian Standards Association, Etobicoke, Ontario, Canada.

CSA (2004), Design of Concrete Structures, A23.3-04, Canadian Standards Association, Mississauga, Ontario, Canada.

Elfegren, L., Karlsson, I. and Losberg, A. (1974), "Torsion-Bending-Shear Interaction for Concrete Beams", *J. Struct. Division ASCE*, **100**(ST8), 1657-1676.

Fang, I.K. and Shiau, J.K. (2004), "Torsional Behavior of Normal- and High-Strength Concrete Beams", *ACI Struct. J.*, **101**(3), 304-313. <http://doi.org/10.14359/13090>.

Goodno, B.J. and Gere, J.M. (2017), *Mechanics of Materials*, Cengage Learning, MA, USA.

Greene, G.G. and Belarbi, A. (2009), "Model for Reinforced Concrete Members under Torsion, Bending, and Shear. I: Theory", *J. Eng. Mech. ASCE*, **135**(9), 961-969. [http://doi.org/10.1061/\(ASCE\)0733-9399\(2009\)135:9\(961\)](http://doi.org/10.1061/(ASCE)0733-9399(2009)135:9(961)).

Hwang, J.H., Lee, D.H., Ju, H., Kim, K.S., Kang, T.H.K. and Pan, Z.F. (2016), "Shear Deformation of Steel Fiber-Reinforced Prestressed Concrete Beams", *J. Concrete Struct. Mater.*, **10**(3), S53-S63. <http://doi.org/10.1007/s40069-016-0159-2>.

Hsu TTC (1968), "Torsion of Structural Concrete-Behavior of

- Reinforced Concrete Rectangular Members”, *Torsion of Structural Concrete. American Concrete Institute*, Farmington Hills, Detroit, USA, ACI Publications SP-18, 261-306. <http://doi.org/10.14359/17572>.
- Hsu, T.T.C. (1984), *Torsion of Reinforced Concrete*, Van Nostrand Reinhold, New York, USA.
- Hsu, T.T.C. (1990), “Shear Flow Zone in Torsion of Reinforced Concrete”, *J. Struct. Eng.*, **116**(11), 3206-3226. [https://doi.org/10.1061/\(ASCE\)0733-9445\(1990\)116:11\(3206\)](https://doi.org/10.1061/(ASCE)0733-9445(1990)116:11(3206))
- Hsu, T.T.C. (1998), “Stresses and Crack Angles in Concrete Membrane Elements”, *J. Struct. Eng. ASCE*, **124**(12), 1476-1484. [https://doi.org/10.1061/\(ASCE\)0733-9445\(1998\)124:12\(1476\)](https://doi.org/10.1061/(ASCE)0733-9445(1998)124:12(1476)).
- Hsu, T.T.C. and Mo, Y.L. (1985), “Softening of concrete in torsional members—Theory and Tests”, *ACI J.*, **82**(3), 290-303. <http://doi.org/10.14359/10335>.
- Hsu, T.T.C. and Mo, Y.L. (1985), “Softening of concrete in torsional members—Design Recommendations”, *ACI J.*, **82**(4), 443-451. <http://doi.org/10.14359/10355>.
- Hsu, T.T.C. and Mo, Y.L. (2010), *Unified Theory of Concrete Structures*, Wiley and Sons, New York, USA.
- Hsu, T.T.C. and Zhang, L.X. (1996), “Tension Stiffening in Reinforced Concrete Membrane Element”, *ACI Struct. J.*, **93**(1), 108-115. <http://doi.org/10.14359/9681>.
- Hsu, T.T.C. and Zhang, L.X. (1997), “Nonlinear analysis of membrane elements by fixed-angle softened-truss model”, *ACI Struct. J.*, **94**(5), 483-492. <http://doi.org/10.14359/498>.
- Hsu, T.T.C. and Zhu, R.R.H. (2002), “Softened Membrane Model for Reinforced Concrete Elements in Shear”, *ACI Struct. J.*, **99**(4), 460-469. <http://doi.org/10.14359/12115>.
- Jeng, C.H. (2015), “Unified Softened Membrane Model for Torsion in Hollow and Solid Reinforced Concrete Members: Modeling Precracking and Postcracking Behavior”, *J. Struct. Eng. ASCE*, **141**(10), 1-20. [https://doi.org/10.1061/\(ASCE\)ST.1943-541X.0001212](https://doi.org/10.1061/(ASCE)ST.1943-541X.0001212).
- Jeng, C.H. and Hsu, T.T.C. (2009), “A Softened Membrane Model for Torsion in Reinforced Concrete Members”, *Eng. Struct.*, **32**(9), 1944-1954. <https://doi.org/10.1016/j.engstruct.2009.02.038>.
- Ju, H., Kim, K.S., Lee, D.H., Hwang, J.H., Choi, S.H. and Oh, Y.H. (2015), “Torsional Responses of Steel Fiber-Reinforced Concrete Members”, *Compos. Struct.*, **129**(1), 143-156. <https://doi.org/10.1016/j.compstruct.2015.04.003>.
- Ju, H., Lee, D.H. and Kim, K.S. (2019), “Minimum Torsional Reinforcement Ratio for Reinforced Concrete Members with Steel Fibers”, *Compos. Struct.*, **207**(1), 460-470. <https://doi.org/10.1016/j.compstruct.2018.09.068>.
- Ju, H., Lee, D., Kim, J.R. and Kim, K.S. (2020), “Maximum Torsional Reinforcement Ratio of Reinforced Concrete Beams”, *Structures*, **23**(1), 481-493. <https://doi.org/10.1016/j.istruc.2019.09.007>.
- Ju, H., Lee, D.H., Hwang, J.H., Kim, K.S. and Oh, Y.H. (2013), “Fixed-Angle Smear-Truss Approach with Direct Tension Force Transfer Model for Torsional Behavior of Steel Fiber-Reinforced Concrete Members”, *J. Adv. Concrete Technol.*, **11**(9), 215-229. <http://doi.org/10.3151/jact.11.215>.
- Koutchoukali, N.E. and Belarbi, A. (2001), “Torsion of High-Strength Reinforced Concrete Beams and Minimum Reinforcement Requirement”, *ACI Struct. J.*, **98**(4), 462-469. <http://doi.org/10.14359/10289>.
- Lee, J.Y. and Kim, S.W. (2010), “Torsional Strength of RC Beams Considering Tension Stiffening Effect”, *J. Struct. Eng. ASCE*, **136**(11), 1367-1378. [https://doi.org/10.1061/\(ASCE\)ST.1943-541X.0000237](https://doi.org/10.1061/(ASCE)ST.1943-541X.0000237).
- Lee, D.H., Han, S.J. and Kim, K.S. (2016), “Dual Potential Capacity Model for Reinforced Concrete Beams Subjected to Shear”, *Struct. Concrete*, **17**(3), 1443-456. <http://doi.org/10.1002/suco.201500165>.
- Lessig, N.N. (1959), “Determination of the Load Carrying Capacity of Reinforced Concrete Elements with Rectangular Cross-Section Subjected to Flexure with Torsion”, *Institute Betona I Zhelezobetona*, Moscow, Work 5, 4-28.
- Lu, J.K. and Wu, W.H. (2001), “Application of Softened Truss Model with Plastic Approach to Reinforced Concrete Beams in Torsion”, *Struct. Eng. Mech.*, **11**(4), 393-406. <https://doi.org/10.12989/sem.2001.11.4.393>.
- McMullen, A.E. and El-Degwy, W.M. (1985), “Prestressed Concrete Tests Compared with Torsion Theories”, *PCI J.*, **30**(5), 96-127. <http://doi.org/10.15554/pci.09011985.96.127>.
- McMullen, A.E. and Rangan, B.V. (1978), “Pure Torsion in Rectangular Sections—A Re-Examination”, *ACI J.*, **75**(10), 511-519. <http://doi.org/10.14359/10963>.
- Mitchell, D. and Collins, M.P. (1974), “Diagonal compression field theory—A rational model for structural concrete in pure torsion”, *ACI J.*, **71**(8), 396-408. <http://doi.org/10.14359/7103>.
- Muttoni, A. and Fernández, R.M. (2008), “Shear Strength of Members without Transverse Reinforcement as a Function of the Critical Shear Crack Width”, *ACI Struct. J.*, **105**(2), 163-172. <http://doi.org/10.14359/19731>.
- Pang, X.B. and Hsu, T.T.C. (1996), “Fixed-angle softened-truss model for reinforced concrete”, *ACI Struct. J.*, **93**(2), 197-207. <http://doi.org/10.14359/1452>.
- Rahal, K.N. (1993), “Behavior of Reinforced Concrete Beams Subjected to Combined Shear and Torsion”, Ph.D. Dissertation, University of Toronto, Ontario, Canada.
- Rahal, K.N. (2001), “Analysis and Design for Torsion in Reinforced and Prestressed Concrete Beams”, *Struct. Eng. Mech.*, **11**(6), 575-590. <https://doi.org/10.12989/sem.2001.11.6.575>.
- Rahal, K.N. (2006), “Evaluation of AASHTO-LRFD General Procedure for Torsion and Combined Loading”, *ACI Struct. J.*, **103**(5), 683-692. <http://doi.org/10.14359/16920>.
- Rahal, K.N. and Collins, M.P. (1995), “Analysis of Sections Subjected to Combined Shear and Torsion—A Theoretical Model”, *ACI Struct. J.*, **92**(4), 459-469. <http://doi.org/10.14359/995>.
- Rahal, K.N. and Collins, M.P. (1996), “Simple Model for Predicting Torsional Strength of Reinforced and Prestressed Concrete Sections”, *ACI Struct. J.*, **93**(6), 658-666. <http://doi.org/10.14359/512>.
- Rahal, K.N. and Collins, M.P. (1999), “Background to the General Method of Shear Design in the 1994 CSA-A23.3 Standard”, *Canadian J. Civil Eng.*, **26**(6), 827-839. <http://doi.org/10.1139/199-050>.
- Sherwood, E.G., Bentz, E.C. and Collins, M.P. (2007), “Effect of Aggregate Size on Beam-Shear Strength of Thick Slabs”, *ACI Struct. J.*, **104**(2), 180-191. <http://doi.org/10.14359/18530>.
- Stevens, N.J., Uzumeri, S.M., Collins, M.P. and Will, G.T. (1991), “Constitutive Model for Reinforced Concrete Finite Element Analysis”, *ACI Struct. J.*, **88**(1), 49-59. <http://doi.org/10.14359/3105>.
- Taylor, H.P.J. (1970), “Investigating of Forces Carried across Cracks in Reinforced Concrete Beams in Shear by Interlock of Aggregate”, TRA 42.447; Cement and Concrete Association, London, United Kingdom. 1-22.
- Tsampras, G., Sause, R., Zhang, D., Fleischman, R., Restrepo, J., Mar, D. and Maffei, J. (2016), “Development of Deformable Connection for Earthquake-Resistant Buildings to Reduce Floor Accelerations and Force Responses”, *Earthq. Eng. Struct. Dynam.*, **45**(9), 1473-1494. <http://doi.org/10.1002/eqe.2718>.
- Vas Rodrigues, R.V., Muttoni, A. and Fernández, R.M. (2010), “Influence of Shear on Rotation Capacity of Reinforced Concrete Members without Shear Reinforcement”, *ACI Struct. J.*, **107**(5), 516-525. <http://doi.org/10.14359/51663902>.
- Vecchio, F.J. (2000), “Disturbed Stress Field Model for Reinforced Concrete: Formulation”, *J. Struct. Eng. ASCE*, **126**(9), 1070-1077. [http://doi.org/10.1061/\(asce\)0733-9445\(2000\)126:9\(1070\)](http://doi.org/10.1061/(asce)0733-9445(2000)126:9(1070)).

- Vecchio, F.J. and Collins, M.P. (1982), "The Response of Reinforced Concrete to In-Plane Shear and Normal Stresses", Department of Civil Engineering, University of Toronto, Ontario, Canada, Publication 82-03, 1-332.
- Vecchio, F.J. and Collins, M.P. (1986), "The Modified Compression Field Theory for Concrete Elements Subjected to Shear", *ACI J.*, **83**(2), 219-231. <http://doi.org/10.14359/10416>.
- Vecchio, F.J. and Collins, M.P. (1988), "Predicting the Response of Reinforced Concrete Beams Subjected to Shear Using Modified Compression Field Theory", *ACI Struct. J.*, **85**(3), 258-268. <http://doi.org/10.14359/2515>.
- Vecchio, F.J. and Collins, M.P. (1993), "Compression Response of Cracked Reinforced Concrete", *J. Struct. Eng. ASCE*, **119**(2), 3590-3610. [http://doi.org/10.1061/\(asce\)0733-9445\(1993\)119:2\(3590\)](http://doi.org/10.1061/(asce)0733-9445(1993)119:2(3590)).
- Walraven, J.C. (1981), "Fundamental Analysis of Aggregate Interlock", *J. Struct. Divison ASCE*, **107**(ST11), 2245-2270.
- Watanabe, F. and Lee, J.Y. (1998), "Theoretical Prediction of Shear Strength and Failure Mode of Reinforced Concrete Beams", *ACI Struct. J.*, **95**(6), 749-757. <http://doi.org/10.14359/588>.
- Wight, J.K. (2015), *Reinforced Concrete Mechanics and Design*, Pearson, New York, USA.
- Zhang, D., Kim, J., Tulebekova, S., Saliyev, D. and Lee, D.H. (2018), "Structural Responses of Reinforced Concrete Pile Foundations Subjected to Pressures from Compressed Air for Renewable Energy Storage", *J. Concrete Struct. Mater.*, **12**(74), 1-16. <http://dor.org/10.1186/s40069-018-0294-z>.

CC

Notations

- A_0 = area enclosed by the centerline of the shear flow zone
- A_c = area enclosed by the outer perimeter of the cross section
- $a_{g,max}$ = maximum size of aggregate
- A_l = amount of longitudinal reinforcement
- A_t = area of one leg of stirrups or amount of transverse reinforcement.
- b = width of the section
- b_v = the effective depth resisting horizontal shear
- c_y = depth of neutral axis
- d_{bl} = diameter of longitudinal steel bar
- d_{bt} = diameter of stirrup steel bar
- d_v = the effective depth resisting vertical shear
- E_s = elastic modulus of steel
- E_{sp} = post-yielding elastic modulus of steel
- f_c = stress-strain relationship of concrete
- f'_c = compressive strength of concrete
- $f_{c,max}$ = softened compressive strength of concrete
- f_l = stress of longitudinal reinforcement
- f_L = stress of longitudinal reinforcement
- f_s = stress of tensile reinforcement
- f_t = stress of transverse reinforcement
- F_L = longitudinal force of the reinforced concrete member under torsion
- f_y = specified yield strength of reinforcement
- f_{ly} = yield stress of longitudinal reinforcement
- f_{ty} = yield stress of transverse reinforcement
- h = height of the section
- jd = flexural moment arm
- K_1 = ratio of the area occupied by the reinforcing bars to the total area along the perimeter of stirrups
- k_c = ratio of average compressive stress to the peak compressive stress in concrete struts
- M = bending moment
- p_0 = perimeter of the shear flow resultant
- p_c = perimeter of the outer concrete cross section
- p_h = perimeter of the centerline of the closed stirrup
- q = shear flow
- s = spacing of transverse reinforcement
- $s_{m\theta}$ = average shear crack spacing
- s_{mx} = average crack spacing that would result if the member was subjected to longitudinal tension
- s_{mv} = average crack spacing that would result if the member was subjected to a transverse tension
- Sp = spalling potential
- T = torsional moment
- t_d = effective thickness of shear flow zone
- w_s = shear crack width
- w_{sh} = effective width resisting horizontal or vertical shear
- α = angle of compression strut with respect to the longitudinal axis
- α_1 = angle of principal stress with respect to the longitudinal axis
- α_2 = angle of initial crack with respect to the longitudinal axis
- β = deviation angle between initial crack angle and principal stress angle
- ϵ_1 = average tensile strain in the 1- direction (initial crack direction)
- ϵ_{cu} = ultimate compressive strain of concrete
- ϵ'_c = maximum strain of concrete at the compressive strength
- ϵ_d = average principal compressive strain
- ϵ_{ds} = maximum principal compressive strain
- ϵ_l = average strain in the l - direction or longitudinal direction
- ϵ_r = average principal tensile strain
- ϵ_t = average strain in the t -direction
- ϵ_{st} = strain of reinforcement

- ε_x = longitudinal strain of member in CSA code
 ε_y = yield strain of steel
 ζ = softening coefficient of concrete in compression
 λ = modification factor for lightweight concrete
 ρ_t = longitudinal reinforcement ratio, taken as $A_t / (t_d p_0)$
 ρ_L = longitudinal reinforcement ratio in gross section, taken as A_L / A_c
 ρ_t = transverse reinforcement ratio, taken as $A_t / (t_d s)$
 ρ_T = transverse reinforcement ratio in gross section, taken as $A_t p_h / (A_c s)$
 σ_{cn} = stress caused by an axial force
 σ_{cap}^c = capacity for concrete crushing
 σ_d = average principal compressive stress in concrete
 σ_l = average normal stress in the longitudinal direction
 σ_r = average principal tensile stress in concrete
 σ_t = average normal stress in the transverse direction
 τ_{21}^c = average shear stress of concrete in the initial crack direction
 τ_{cap}^{ci} = shear resistance capacity due to aggregate interlock
 τ_h = average shear stress in the $l-t$ coordinate